

# SEGMENTATION OF RETINAL BLOOD VESSELS BASED ON ANALYSIS OF THE HESSIAN MATRIX AND CLUSTERING ALGORITHM

Nancy M. Salem, Sameh A. Salem, and Asoke K. Nandi

Signal Processing and Communications Group,  
Department of Electrical Engineering and Electronics,  
The University of Liverpool, Brownlow Hill, L69 3GJ, Liverpool, U.K.  
phone: +44 151 794 4525, fax: +44 151 794 4540, email: {nancy.salem, sameh.salem, a.nandi} @liv.ac.uk

## ABSTRACT

In this paper, a novel unsupervised method to segment retinal blood vessels from colour fundus images is proposed. A new vesselness measure is introduced which is based on detecting vessel centerlines and orientation in scale space. Based on this vesselness measure a generated ground truth (GGT) image is obtained by thresholding and removing segments of small sizes. The segmentation is obtained by using this GGT image in conjunction with a RAdius-based Clustering Algorithm (RACAL). A dataset of 20 images publicly available is used to evaluate the performance of our proposed method. Experimental results show that a true positive rate (TPR) of 81% at false positive rate (FPR) of 4.5% is achieved compared with TPR of 76% at the same FPR from the piecewise threshold probing method [1].

## 1. INTRODUCTION

Automated analysis of retinal images is a challenging research area that aims to provide automated methods to help in the early detection and diagnosis of many eye diseases such as diabetic retinopathy and age-related macular degeneration (AMD).

Automated segmentation of retinal blood vessels is an important step in screening programs for diabetic retinopathy [2], evaluation of the retinopathy of prematurity [3], registration of retinal images for treatment evaluation [4], generating retinal map for the diagnosis and treatment of AMD [5], or locating the optic disc [6] and the fovea.

Retinal blood vessels segmentation methods, according to the classification method, can be divided into two groups - supervised and unsupervised methods [7]. Unsupervised methods in the literature comprise the matched filter response [1], grouping of edge pixels [5], adaptive thresholding [8, 9], vessel tracking [9, 10], topology adaptive snakes [11], and morphology-based techniques [12]. Supervised methods are the most recent approaches in vessel segmentation and use the neural networks [2], the  $K$ -nearest neighbour classifier [7], or the Bayesian classifier [13] for classifying image pixels as blood vessel or non-blood vessel pixels. These methods depend on generating a feature vector for every pixel in the image and then using training samples (with known classes) to design a classifier to classify these training samples into their corresponding classes.

In this paper, we introduce an unsupervised method for segmentation of retinal blood vessels from colour fundus images. Blood vessels centerlines and orientation are used to measure the vesselness, then by removing segments of small sizes an image that represent blood vessels is obtained,

which we call generated ground truth (GGT) image. Next, a feature vector of three features is used in conjunction with RACAL algorithm [14] to cluster image pixels into clusters. Finally, these clusters are classified as vessels or non-vessels using the GGT image. The main advantage of our proposed method is that it is completely unsupervised, so there is no need for manually labeled images which is time consuming and require an expert.

## 2. PROPOSED SEGMENTATION METHOD

### 2.1 Preprocessing of Retinal Images

Unsupervised methods for segmenting blood vessels in colour fundus images use the green channel [1, 7, 8, 15] because generally it has the highest contrast between blood vessels and the retinal background while the red channel is rather saturated and the blue channel is rather dark.

For efficient segmentation of retinal blood vessels, it is desirable to have high contrast between the retinal blood vessels and retinal background whilst there should be low contrast between retinal background and retinal abnormalities. Combining the advantages of both channels, brightness in red channel and high contrast in green channel, results in decreasing the contrast between the abnormalities and the retinal background. This helps to reduce some responses, which do not resemble to any blood vessels and that would otherwise decrease the performance of blood vessels segmentation methods.

Histogram matching is an approach that is used to generate a processed image that has a specified histogram, it has the advantage of producing more realistic looking images than those generating by equalisation. We use the concept of histogram matching to modify the histogram of the green channel image using that of the red channel image in order to combine the distributions of gray-levels of both images [16]. Figure 1 shows the effect of this preprocessing step using two test images.

### 2.2 Vesselness Measure

Blood vessels can be considered as dark elongated or line structures - of different diameters and orientations - on a brighter background. Our proposed vesselness measure is based on detecting vessel centerlines and orientation over scales. The large eigenvalue of the Hessian matrix is used as an indicator of the vessel centerline. As vessels are of different diameters, then different scales are used to calculate the eigenvalues and then keeping the maximum response at each image pixel over scales.

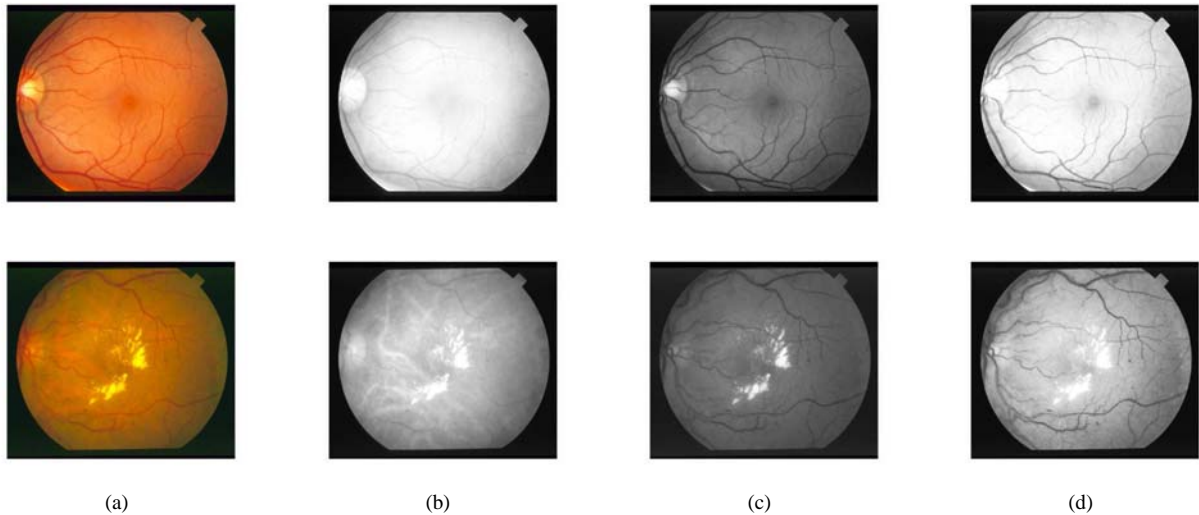


Figure 1: Preprocessing step for normal (top) and abnormal (bottom) images. (a) colour image, (b) red channel, (c) green channel, and (d) histogram matched images.

The appropriate local coordinate system in case of line structures is defined by the eigenvectors of the Hessian matrix, matrix of the second order derivatives of the intensity image  $L(x, y)$ . Image derivatives can be taken by convolving the image with derivatives of Gaussian using the Gaussian scale-space techniques [17].

$$L_{xj} = \frac{\partial L(\mathbf{x}, \sigma)}{\partial x_j} = \frac{1}{2\pi\sigma^2} \int_{\mathbf{x}' \in \mathbb{R}^2} \frac{\partial e^{-\|\mathbf{x}-\mathbf{x}'\|^2/2\sigma^2}}{\partial x_j} L(\mathbf{x}') d\mathbf{x}' \quad (1)$$

where  $x_j$  is the image coordinate with respect to which the derivative is taken. Mixed and higher order derivatives are computed by taking mixed and higher order derivatives of the Gaussian kernel.

Eigenvalues (the large eigenvalue,  $\lambda_+$ , and the small eigenvalue,  $\lambda_-$ , where  $\lambda_+ > \lambda_-$ ) of the Hessian matrix of the intensity image  $L(x, y)$  are calculated as [18]:

$$\lambda_+ = \frac{L_{xx} + L_{yy} + \alpha}{2} \quad (2)$$

$$\lambda_- = \frac{L_{xx} + L_{yy} - \alpha}{2} \quad (3)$$

where  $L_{xx}$ ,  $L_{yy}$  are the second derivatives of the intensity image in  $x$ - and  $y$ - directions, and  $\alpha = \sqrt{(L_{xx} - L_{yy})^2 + 4L_{xy}^2}$ . Then, the local maximum of the large eigenvalue  $\lambda_{max}$  is calculated as :

$$\lambda_{max} = \max_s [\lambda_+(s)] \quad (4)$$

Figure 2 shows eigenvectors corresponding to large and small eigenvalues at different scales. Orientation from the eigenvector that corresponds to the small eigenvalue shows the direction of the vessels, while the orientation from the eigenvector that corresponds to the large eigenvalue shows the direction of the large changes in the intensity values

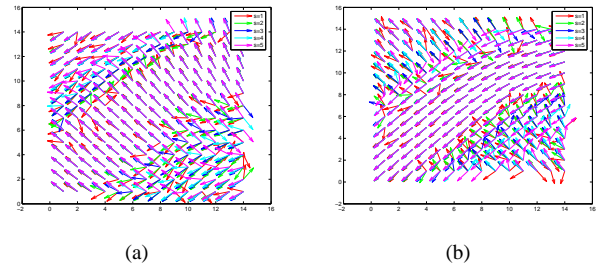


Figure 2: Eigenvectors (blood vessel orientation) corresponding to (a) large eigenvalues, and (b) small eigenvalues at different scales .

which represents the perpendicular direction to the vessel.

Vessel orientation in angles,  $\theta$ , are calculated from the eigenvectors of the Hessian matrix as:

$$\hat{e}_+ = \frac{1}{N} \begin{vmatrix} 2L_{xy} \\ L_{yy} - L_{xx} + \alpha \end{vmatrix} \quad (5)$$

$$\hat{e}_- = \frac{1}{N} \begin{vmatrix} L_{yy} - L_{xx} + \alpha \\ -2L_{xy} \end{vmatrix} \quad (6)$$

$$\theta_+ = \tan^{-1} \left[ \frac{L_{yy} - L_{xx} + \alpha}{2L_{xy}} \right] \quad (7)$$

$$\theta_- = \tan^{-1} \left[ \frac{-2L_{xy}}{L_{yy} - L_{xx} + \alpha} \right] \quad (8)$$

where  $\hat{e}_+$ ,  $\theta_+$ ,  $\hat{e}_-$  and  $\theta_-$  are the eigenvectors and  $\theta$  corresponding to  $\lambda_+$ ,  $\lambda_-$  and  $N = \sqrt{(L_{yy} - L_{xx} + \alpha)^2 + 4L_{xy}^2}$ .

What has been observed from our experiments is that as the scale parameter value increases so does the apparent diameter of the detected blood vessel. This can be clearly appreciated from Fig. 3 which displays a sub-image and the

corresponding sub-images containing the large eigenvalue at every pixel at six different scales.

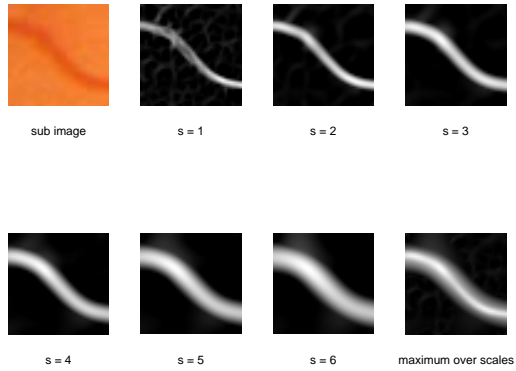


Figure 3: The large eigenvalue for a retinal blood vessel at different scales.

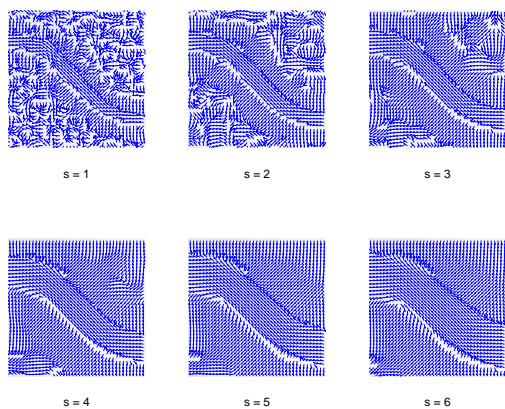


Figure 4: Eigenvectors at different scales

Directions of eigenvectors corresponding to the small eigenvalue at each pixel are depicted in the sub-image for six different scales in Fig. 4. It has also been observed that the variation of the directions of the eigenvectors in a pixel over six different scales is smaller for blood vessel pixels compared with non-blood vessel pixels.

We use the standard deviation of orientation values over scales as a measure of vessel orientation variation over scales. At vessel centers, the standard deviation of  $\theta_-$ , angle with respect to  $x$ -axis calculated from the eigenvector that corresponds to small eigenvalue  $\lambda_-$ , over scales tends towards zero, or a very small value, compared with higher values outside blood vessels. Figure 5 shows the probability density function of the standard deviation values of  $\theta_-$  over scales calculated for vessel and non-vessel pixels in a sub image.

The standard deviation of  $\theta_-$  over scales is calculated as:

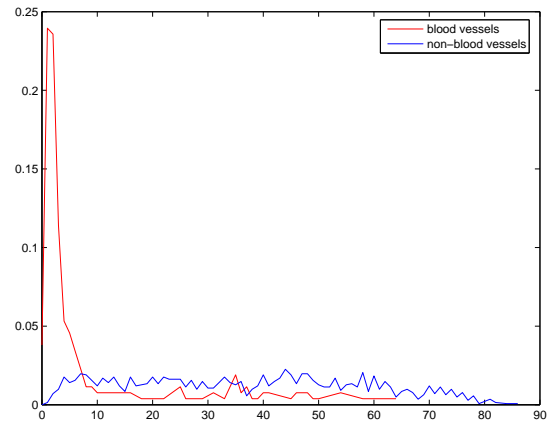


Figure 5: Probability density function of the standard deviation values of  $\theta_-$  over scales for vessel and non-vessel pixels.

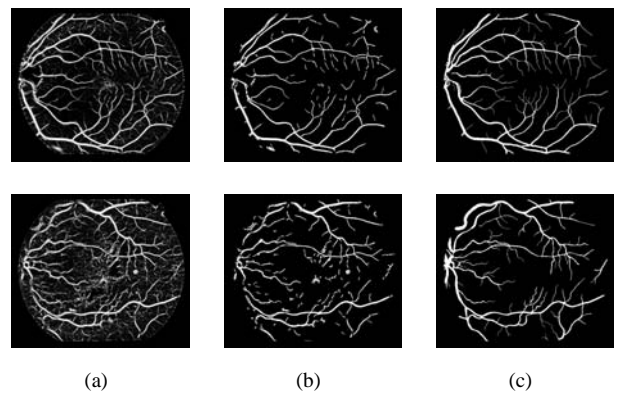


Figure 6: (a) Vesselness measure, (b) GGT image, and (c) ground truth (manually labeled) for a normal (top) and abnormal (bottom) images.

$$\theta_{std} = \frac{std[\theta_-(s)]}{s} \quad (9)$$

The proposed vesselness measure  $V$  is calculated as :

$$V = \frac{\lambda_{max}}{\theta_{std} + \epsilon} \quad (10)$$

where  $\lambda_{max}$  is the local maximum of the large eigenvalue over scales,  $\theta_{std}$  is the standard deviation of the  $\theta_-$  over scales, and  $\epsilon$  is a small value to avoid singularities. The GGT image is obtained from the vesselness measure after thresholding and removing segments of sizes smaller than 30 pixels, these images are shown in Fig. 6 with the manually labeled image (ground truth) by the human observer.

### 2.3 Clustering Procedure

A feature vector for each image pixel is generated, then these features are used to cluster image pixels to a number of non-overlapped clusters. GGT image is used as known labels for clustered pixels in order to classify each cluster to its corresponding class (vessel or non-vessel).

In the clustering step we use the RACAL algorithm [14], which is a RAdius-based Clustering ALgorithm (*RACAL*), that uses a distance based principle to map the distributions of the pixels in feature space by utilising the premise that clusters are determined by a distance parameter (without having to specify the number of clusters). Simply expressed, RACAL defines a normalised distance parameter,  $\delta_o$  ( $0 \leq \delta_o \leq 1$ ), which acts as the determinant of the cluster. From a given object (pixel) which is characterised by  $p$  features, any other objects that fall within  $\delta_o$  are regarded as belonging to the same cluster. The control of the cluster size is achieved through the manipulation of  $\delta_o$  parameter. Small values will lead to a high number of small, tight clusters, and large values of  $\delta_o$  will create a smaller number of larger clusters, while extremely large values will cause only one cluster to be formed.

The feature vector used with RACAL consists of colour and scale-space features. Based on the property that a blood vessel can be seen in the colour retinal image as a dark object on a brighter background, from the three colour channels (red, green and blue) the green channel is chosen to represent this characteristic as it has the highest contrast between blood vessels and the retinal background. The two characterising attributes of any vessel, i.e. piecewise linearity and parallel edges [19], are considered when choosing the set of features for every pixel in retinal images. The piecewise linear property of a blood vessel can be recognised by extracting centerlines of blood vessels, simply by extracting the image ridges. The parallel edges property is well recognised by calculating the gradient magnitude of the image intensity. Because the vessels are of different diameters, so these features are extracted at different scales and then the local maximum over scales is calculated for both features as in Eqs. 12 and 13.

$$Feat1 = \text{Green channel image} \quad (11)$$

$$Feat2 = \max_s \left[ \frac{|\nabla L(s)|}{s} \right] \quad (12)$$

where  $|\nabla L| = \sqrt{L_x^2 + L_y^2}$

$$Feat3 = \max_s \left[ \frac{\lambda_+(s)}{s} \right] \quad (13)$$

These three features were normalised to zero mean and unit standard deviation.

### 3. DATASET

For performance evaluation, a publicly available dataset [20] consists of 20 images which are digitized slides captured by a TopCon TRV-50 fundus camera at  $35^\circ$  FOV. Each slide was digitized to produce a  $605 \times 700$  pixels image, standard RGB, 8 bits per colour channel. Every image has been manually segmented by two observers to produce ground truth vessels segmentation. Ten of these images contain pathology and the other ten are normal, giving a good opportunity to test the proposed method in both normal and abnormal retinas.

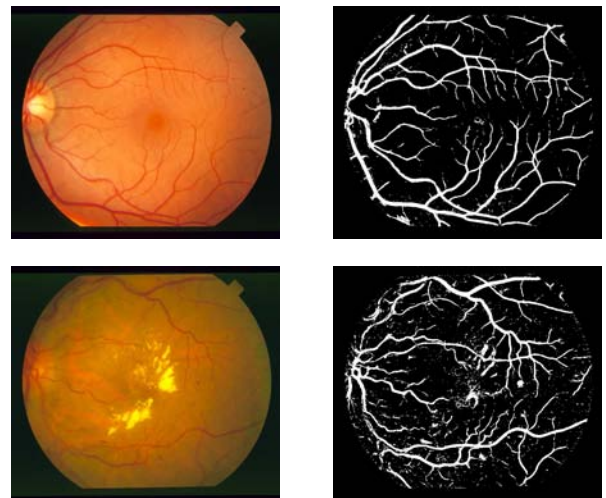


Figure 7: Segmentation results using RACAL algorithm.

Table 1: Clustering results (average for 20 images)

Image Type	FPR %	TPR %
Normal	3.36	84.22
Abnormal	5.64	77.56
All images	4.5	80.89

### 4. RESULTS AND DISCUSSION

In our experiments, each image is preprocessed using the histogram matching to reduce the contrast between abnormalities and the retinal background. Then the vessellness measure is used for vessel segmentation by finding the local maximum of the large eigenvalue and the standard deviation of vessel orientations at different scale values, as in Eq.10. The GGT image is obtained by thresholding and removing segments of size less than 30 pixels. In the clustering step; the RACAL is used with a feature vector, of three features, to cluster image pixels to a number of non-overlapped clusters. The final segmentation is achieved by finding the corresponding class of each of the obtained clusters based on labeled pixels from the GGT image, as shown in Fig. 7.

The performance is measured with Receiver Operating Characteristic (ROC) curves. An ROC curve plots the false positive rates against the true positive rates, and these rates are defined in the same way as in [1].

Results after the clustering step are summarised in Table 1, while Table 2 shows segmentation results for other methods [1, 8, 9]. On average, for the 20 images in the dataset, a TPR of 81% is achieved at FPR of 4.5% by our proposed method compared with TPR of 76% by the piecewise threshold probing method [1] at the same FPR.

It is important to note that in [1, 8], there are five parameters required for these two algorithms, and the reported results are for processing all the 20 images in the STARE dataset using ten and eight sets of values for these parameters respectively. While in [9], as it uses a vessel tracing technique so it is affected by incorrectly identified initial tracing points also it requires manually labeled images

Table 2: Performance of vessel segmentation methods using STARE images

Method	FPR	TPR
2nd Human observer	4.4	89.5
Wu [9]	3.9	84.3
Jiang [8]	4.4	83.5
Hoover [1]	4.5	75.8
proposed method	4.5	80.9

for training the parameters, (one for normal and one for abnormal images). Significantly, for our proposed algorithm, we need to set one parameter only, which is the  $\delta_0$  for the RACAL,  $\delta_0 = 0.04$  is chosen after some exploratory experiments. To generate the GGT images we threshold the image results from the proposed vesselness measure at threshold = 0.5.

One of the main advantages of the proposed method, it is completely unsupervised, so there is no need for manually labeled images, segmented by a human observer, which is time consuming and subject to the observer. Results can be enhanced by introducing a post processing step to reduce number of false positives depending on a set of features such as: pixel's intensity information, segment's (region) size, probability of belonging to a blood vessel, and segment's mean intensity. Further investigations are under way in the post-processing step.

## 5. CONCLUSIONS

A novel unsupervised method for retinal blood vessels segmentation is proposed. This method is based on a vesselness measure, which depends on vessel centerlines and orientation, in conjunction with RACAL algorithm. As demonstrated, at 4.5% FPR, retinal blood vessels have been segmented using the proposed unsupervised method with TPR of 81%, our results can be improved when introducing a post processing step to reduce false positives.

## 6. ACKNOWLEDGMENT

The authors would like to thank A. Hoover for making the retinal images publicly available. N.M. Salem and S.A. Salem would like to acknowledge the financial support of the Ministry of Higher Education, Egypt, for this research.

## REFERENCES

- [1] A. Hoover, V. Kouznetsova, and M. Goldbaum, "Locating blood vessels in retinal images by piece-wise threshold probing of a matched filter response," *IEEE Transactions on Medical Imaging*, vol. 19, pp. 203–210, Mar. 2000.
- [2] C. Sinthanayothin, J. F. Boyee, T. H. Williamson, H. L. Cook, E. Mensah, S. Lal, and D. Usher, "Automated detection of diabetic retinopathy on digital fundus images," *Diabetic Med.*, vol. 19, no. 2, pp. 105–112, 2002.
- [3] C. Heneghan, J. Flynn, M. O'Keefe, and M. Cahill, "Characterization of changes in blood vessel width and tortuosity in retinopathy of prematurity using image analysis," *Medical Image Analysis*, vol. 6, pp. 407–429, Dec. 2002.
- [4] F. Zana and J. Klein, "A multimodal registration algorithm of eye fundus images using vessel detection and Hough transform," *IEEE Transactions on Medical Imaging*, vol. 18, pp. 419–428, May 1999.
- [5] A. Pinz, S. Bernögger, P. Daltinger, and A. Kruger, "Mapping the human retina," *IEEE Transactions on Medical Imaging*, vol. 17, pp. 606–619, Aug. 1998.
- [6] A. Hoover and M. Goldbaum, "Locating the optic nerve in a retinal image using fuzzy convergence of the blood vessels," *IEEE Transactions on Medical Imaging*, vol. 22, pp. 951–958, Aug. 2003.
- [7] J. Staal, M. D. Abràmoff, M. Niemeijer, M. A. Viergever, and B. van Ginneken, "Ridge-based vessel segmentation in color images of the retina," *IEEE Transactions on Medical Imaging*, vol. 23, pp. 501–509, April 2004.
- [8] X. Jiang and D. Mojon, "Adaptive local thresholding by verification-based multithreshold probing with application to vessel detection in retinal images," *IEEE Transactions on Pattern Analysis and Machine Intelligent*, vol. 25, pp. 131–137, Jan. 2003.
- [9] D. Wu, M. Zhang, J. Liu, and W. Bauman, "On the adaptive detection of blood vessels in retinal images," *IEEE Transactions on Biomedical Engineering*, vol. 53, no. 2, pp. 341–343, Feb. 2006.
- [10] Y. A. Tolias and S. M. Panas, "A fuzzy vessel tracking algorithm for retinal images based on fuzzy clustering," *IEEE Transactions on Medical Imaging*, vol. 17, pp. 263–273, April 1998.
- [11] T. McInerney and D. Terzopoulos, "T-snakes: topology adaptive snakes," *Medical Image Analysis*, vol. 4, no. 2, pp. 73–91, 2000.
- [12] F. Zana and J. C. Klein, "Segmentation of vessel-like patterns using mathematical morphology and curvature evaluation," *IEEE Transactions on Image Processing*, vol. 10, no. 7, pp. 1010–1019, July 2001.
- [13] J. V. B. Soares, J. J. G. Leandro, R. M. Cesar-Jr., H. F. Jelinek, and M. J. Cree, "Retinal vessel segmentation using the 2-D Gabor wavelet and supervised classification," *IEEE Transactions on Medical Imaging*, vol. 25, pp. 1214–1222, 2006.
- [14] S. A. Salem and A. K. Nandi, "Novel clustering algorithm (RACAL) and a partial supervision strategy for classification," in *IEEE International Workshop on Machine Learning for Signal Processing*, Mynooth, Ireland, 6–8 Sept. 2006, pp. 313–318.
- [15] S. Chaudhuri, S. Chatterjee, N. Katz, and M. Goldbaum, "Detection of blood vessels in retinal images using two-dimensional matched filters," *IEEE Transactions on Medical Imaging*, vol. 8, pp. 263–269, Sept. 1989.
- [16] N. M. Salem and A. K. Nandi, "Novel pre-processing of colour retinal images," in *3rd IEE International Seminar on Medical Applications of Signal Processing*, London, UK, 3–4 Nov. 2005.
- [17] T. Lindeberg, *Scale-space Theory in Computer Vision*, Kluwer Academic publisher, Netherlands, 1994.
- [18] M. E Martínez-Pérez, A. Hughes, A. Stanton, S. Thom, A. Bharath, and K. Parker, "Scale-space analysis for the characterisation of retinal blood vessels," in *Medical Image Computing and Computer-Assisted Intervention - MICCAI '99*, C. Taylor and A. Colchester, Eds., 1999, pp. 90–97.
- [19] J. J. Kanski, *Clinical Ophthalmology: A systematic approach*, Butterworth-Heinemann, Oxford, 4th edition, 1999.
- [20] "The STARE project," Available at: <http://www.ces.clemson.edu/~ahoover/stare>.